Measurement of the Pfirsch-Schlüter and Bootstrap Currents in HSX

J.C. Schmitt, J.N. Talmadge, P.H. Probert, D.T. Anderson

HSX Plasma Laboratory, Univ. of Wisconsin – Madison, WI USA

The Helically Symmetric Experiment is a quasi-helically symmetric axis stellarator that, to a good approximation, has no toroidal curvature. The helical axis of symmetry in |B| and lack of toroidal curvature results in a Pfirsch-Schlüter current that rotates as a function of toroidal angle. Also, the magnitude of this current is reduced by a factor of $1/|n-m\iota| \approx 1/3$ in HSX. Another consequence of the helical axis is that the bootstrap current flows in the direction opposite to that in a tokamak and acts to reduce the rotational transform. These currents are measured in HSX by an external Rogowski coil and an external dB/dt pickup coil array. A 10-chord Thomson scattering system measures the radial profiles of the electron temperature and density. Ion profiles are assumed. Two numerical codes, VMEC and BOOTSJ, calculate the equilibrium MHD current densities and bootstrap current densities in HSX. An additional code, V3FIT, calculates the magnetic field due to the main magnetic field and plasma currents. Comparisons of numerical estimates and recent measurements are presented for 1 Tesla QHS plasmas heated by 50 kW ECRH. The helical nature of the Pfirsch-Schlüter current is confirmed, and the bootstrap current, as calculated by BOOTSJ provides a good estimate of the toroidal current measured in HSX.

Keywords: boostrap current, Pfirsch-Schlüter current, HSX, VMEC, BOOTSJ, V3FIT

1. Introduction

The Helically Symmetric Experiment (HSX), is the world's first stellarator that has an axis of symmetry in |B| [1]. For HSX, $|B| = B_0\left[1-\varepsilon_h \cos\left((n-m\iota)\phi\right)\right]$, with n = 4, m = 1, $\iota \approx 1$ and the toroidal and poloidal angles, ϕ and θ, are related by $\theta = \iota\phi$ in a straight line coordinate system. In Boozer coordinates [2], this can be written as $|B| = B_0 \sum b_{nm} \cos\left(n\alpha_B - m\zeta_B\right)$, with toroidal angle, α_B, poloidal angle, ζ_B, toroidal and poloidal Fourier spectral numbers, n and m, and the amplitude of the spectral component, b_{nm}. For standard plasmas generated with the main field coil set of HSX, the vacuum magnetic field spectrum is dominated by the $(n,m) = \{(0,0),(4,1)\}$ terms, which are the mean background and dominant helical axis terms, and has almost no toroidal curvature, $b_{01} \approx 0$.

One consequence of the helical axis of symmetry is that the Pfirsch-Schlüter current rotates helically with |B| around the machine. Another consequence is a reduction in the magnitude of the Pfirsch-Schlüter current. Consider the following expression for the Pfirsch-Schlüter current [3].

$$J_{PS} = \frac{1}{B_0}\frac{dp}{d\psi} * \sum_{(n,m)\neq(0,0)} \frac{nI+mg}{n-m\iota}\delta_{nm}\cos\left(n\alpha_B - m\zeta_B\right) \qquad (1)$$

The magnitude of the dominant helical term is reduced by a factor of $n - m\iota \approx 3$.

Two significant differences in the bootstrap current exist in HSX compared to that in conventional toroidal fusion experiments. First, the direction of the bootstrap current is opposite to that in a tokamak. This leads to an effective decrease in the rotational transform. An expression for the bootstrap current for the case of one dominant Fourier component [4] also demonstrates the reduction of the dominant term by a factor of $n - m\iota \approx 3$.

$$J_{BS} \propto \frac{1}{B_0}\sqrt{b_{nm}}\,\frac{m}{n-m\iota}\left[gradients\right] \qquad (2)$$

2.1 Diagnostics

The radial profiles of the electron temperature and density of the plasma are measured by a 10-chord Thomson Scattering system. Figures 1 and 2 show several radial profiles of electron temperature and density that have been achieved in 1-Tesla QHS hydrogen plasmas, a standard operating regime for HSX.

Changes in the net toroidal plasma current in HSX are measured with a Rogowski coil which is mounted on the external side of the vacuum vessel. The vessel effectively filters magnetic fluctuations above 5 kHz, and the signal is further filtered at 3.1 kHz and amplified by 18.3 kV-sec/A.

author's e-mail: jcschmitt@wisc.edu

The signal is digitized at 200 kHz, digitally stored and numerically integrated. Figure 3 shows the measured time-evolution of the toroidal current

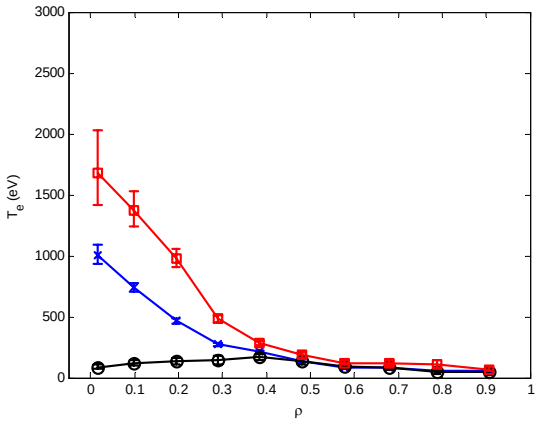

Fig. 1. Electron temperature radial profiles. The various profiles are achieved by varying the electron-cyclotron resonance heating location. ECRH power ~ 44 kW (launched).

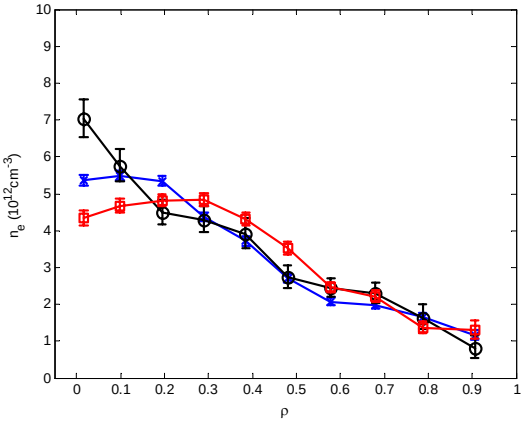

Fig. 2. Electron density profiles. The line-averaged central density is $4.7 \pm 0.3 \times 10^{18}\ cm^{-3}$ in each case.

The toroidal current is seen to reach steady state only in cases where the electron temperature is low. This is shown in figure 3. The collisionality, $\nu_{*e} = \left(\nu_e / \varepsilon_h\right) \Big/ \left(\varepsilon_h^{1/2} v_{Te} / R\, q_{eff}\right)$ and magnetic diffusivity, $\eta_{\parallel} / \mu_0$ are shown in figures 4 and 5. Most QHS plasmas are in the long mean free path regime, and the magnetic diffusivity varies greatly across the plasma.

In addition to the Rogowski coil, there is an array of 16 dB/dt triplets, which provide a measurement of the magnetic field vector due to both the main field coils and plasma currents. Measurements of similar plasma discharges have been performed with the array at two toroidal locations, approximately 1/3 field period apart.

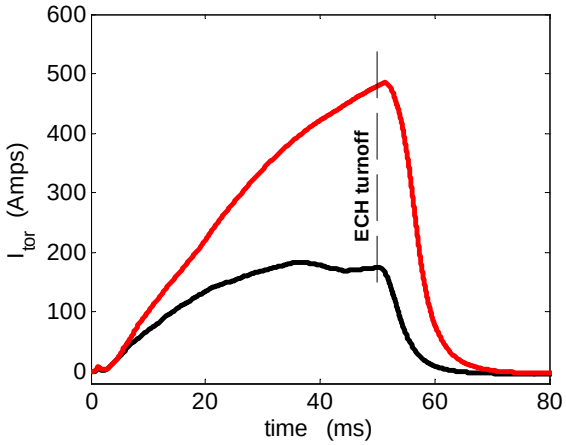

Fig. 3. Time evolution of the toroidal current. Heating resonance: off-axis (black) , near-axis (red).

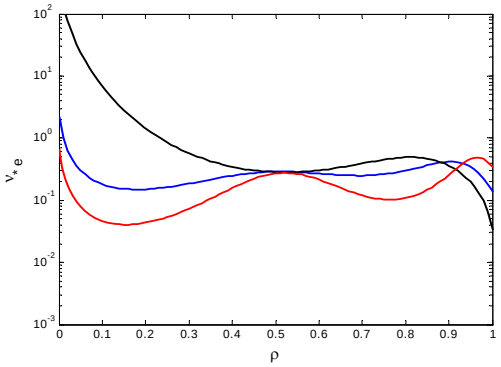

Fig. 4. Electron collisionality.

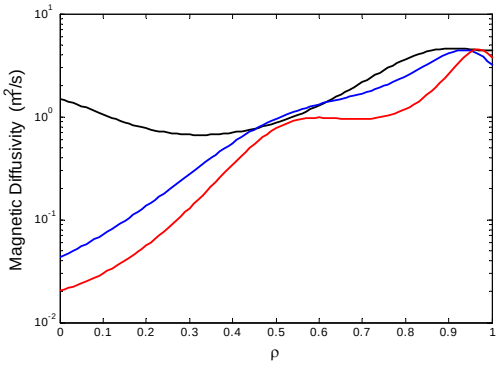

Fig. 5. Magnetic diffusivity.

2.2 Computational Modeling

The free-boundary MHD equilibrium solver, VMEC [5], is used to establish the equilibrium parameters. Measured profiles of electron temperature and density, along with assumed profiles of ion temperature and density $\left(T_i \le T_e / 10 \quad Z_i = 1\right)$ are used to determine the pressure profile for VMEC. After VMEC calculates the equilibrium, the output is used in the BOOTSJ program to calculate the bootstrap current density [6]. VMEC is then re-run with the toroidal current density set equal to the density calculated by BOOTSJ. Further iterations of

BOOTSJ and VMEC could be performed, but the current densities have not been seen to vary much after a single iteration.

The output from VMEC is then fed into V3FIT, which calculates the magnetic response due to currents in the plasma and those due to the main field coils [7]. The response is calculated at the position of each dB/dt triplet.

3.1 Pfirsch-Schlüter Current

The Pfirsch-Schlüter current density in a typical QHS plasma discharge is shown in figure 6. Two toroidal positions are shown, corresponding to the approximate location of the 16 triplets.

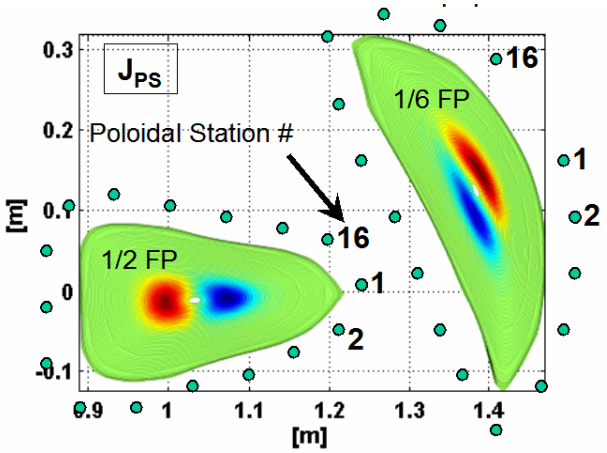

Fig. 6. Pfirsch-Schlüter current density at two toroidal locations and a sketch of the location of the dB/dt triplets.

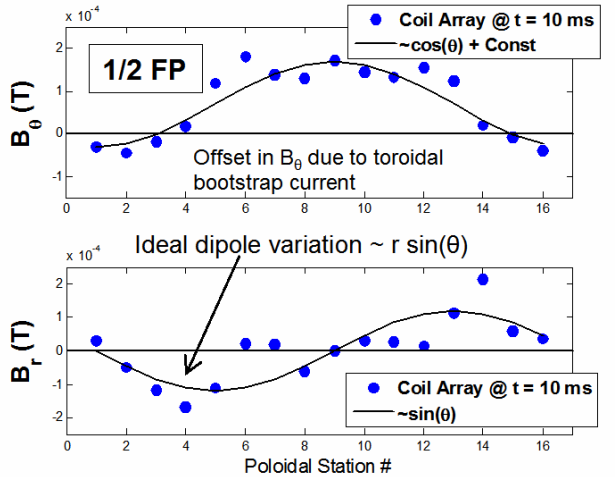

Fig. 7. Measured poloidal and radial magnetic fields at 16 poloidal stations.

The approximately 'poloidal' and 'radial' components of the measured magnetic at each triplet location for the 1/2 field period location is shown in figure 7. This is for a time of t = 10 ms into the plasma discharge, before the bootstrap current has risen to a large value. Two additional sinusoidal lines are sketched, representing the expected response from a cylindrical dipole current for a set of detectors at a constant radial distance from the plasma. The comparison agrees qualitatively, but there are significant differences, in particular for the poloidal stations nearest to (5, 6, 12, 13) and farthest from (9, 11) the plasma column. There is a slight offset in the poloidal comparison, due to the non-zero bootstrap current.

3.2 Bootstrap Current

The expected steady-state value of the bootstrap current for many profiles has been calculated by the use of VMEC and BOOTSJ. These values are then compared to the total toroidal current measured in HSX at the end of the plasma discharge, and a projected steady-state value, I_∞, which is determined by a best-fit of the measured current to the expression $I(t) = I_\infty\left(1 - e^{-t/\tau_{Tor}}\right)$. These two comparisons are shown in figure 8.

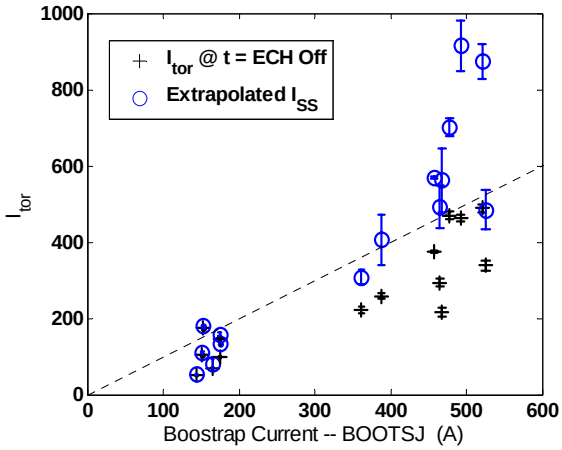

Fig. 8. Measured and projected values of total bootstrap current vs. estimated bootstrap current. Estimate is calculated by BOOTSJ.

The measurements of the toroidal current are consistent with numerical estimates of the bootstrap current. There are several cases where the toroidal current appears to be growing to a larger value than is expected from the calculation, but the discharge had ended before the steady-state had been reached. To date, the estimate of the bootstrap current provides an upper-limit to the measured toroidal current in 1-T QHS plasmas.

4. Temporal Evolution

The time-evolution of the toroidal current, stored energy and line-averaged central electron density are shown in figure 9. The electron pressure and density profiles are captured 0.5 ms before ECH turn-off, when the Thomson Scattering laser fired, and these profiles are shown in figures 1 and 2 as the highest central-T_e (red) line. The total steady-state bootstrap current is estimated by BOOTSJ to be 478 A. The measured toroidal current

reaches 450 A at the end of the discharge, and is projected to be about 710 A in steady state.

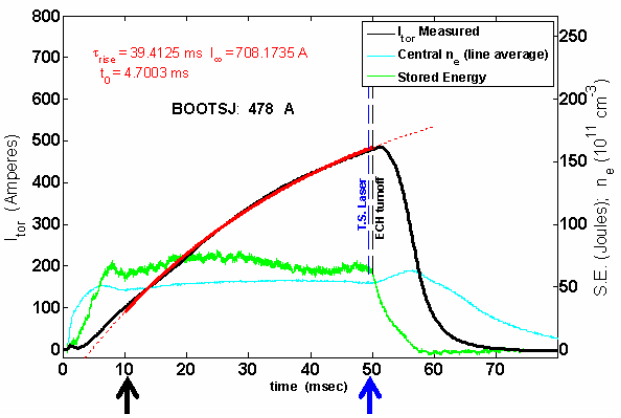

Fig. 9. Time evolution of toroidal current, stored energy, and line-averaged central n_e

The pressure and toroidal current density profiles (from BOOTSJ) used in VMEC are shown in figure 10. The pressure profile is centrally peaked and the bootstrap current is largest at the location of the steep pressure gradient. The rotational transform is altered from the vacuum case, approaching a value of $\iota \approx 1$ near s = 0.15.

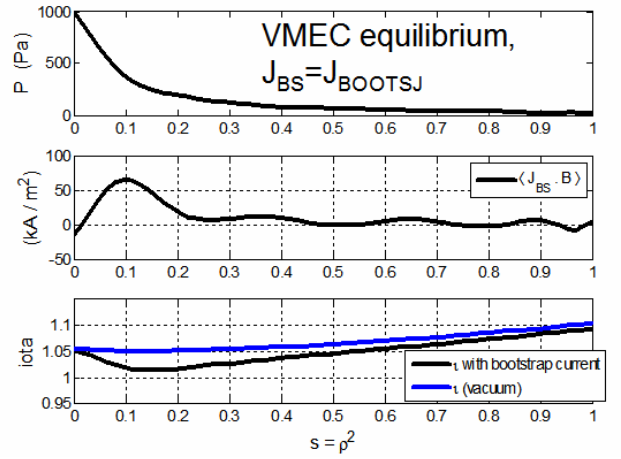

Fig. 10. Radial (VMEC 's') profiles of plasma pressure, bootstrap current and rotational transform. The vacuum transform is also shown.

The measured poloidal and radial magnetic fields due to the plasma current are shown for t = 10 ms and 50 ms for two different toroidal locations (figure 6) in figures 11 and 12. V3FIT was used to calculate the expected magnetic field for two cases: $I_{tor} = 0$ and $I_{tor} = I_{BS}$. These two cases roughly correspond to the situation early in the discharge (small bootstrap current) and late in the discharge (near-steady state current). The calculated magnetic field at the location of each triplet is shown in the figure.

There is considerable agreement between the measured and calculated magnetic fields due to the plasma current. Note that the toroidal current is still evolving, and no information is known about its true radial profile.

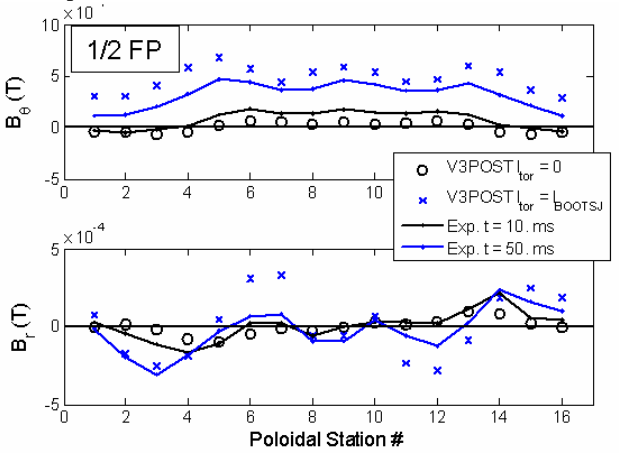

Fig. 11. Magnetic diagnostic responses, measured and calucated (V3FIT results marked as V3POST).
Toroidal location = 1/2 field period.

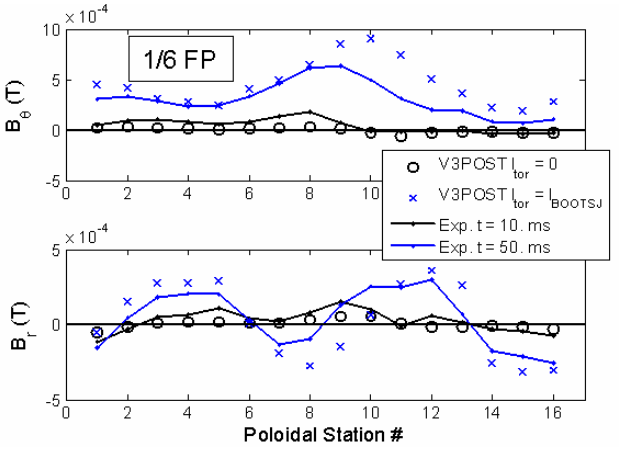

Fig. 12. Magnetic diagnostic responses at a toroidal location of 1/6 field period.

5. Special Thanks

The authors would like to thank the V3FIT team, and especially Steve Knowlton for invaluable contributions and for the V3FIT results that are shown here.

[1] F.S.B.Anderson, A.F.Almagri, D.T.Anderson, P.G.. Mathews, J.N.Talmadge, and J.L.Shohet, Fusion Technol. **27**, 273 (1995).
[2] A.H. Boozer, Phys. Fluids **25**, 520, (1982).
[3] A.H. Boozer, Phys. Fluids **24**, 1999, (1981).
[4] A.H. Boozer and H.J. Gardner, Phys. Fluids B **2**, 2408, (1990).
[5] S.P. Hirshman, W.I. van Rij and P. Merkel, Comp. Physics Comm. **43**, 143 (1986).
[6] Shaing, et. al, Phys. Fluids B **1**, 148 (1989).
[7] S.P. Hirshman, et. al, Physics of Plasmas, **11**, 595 (2004).